



Biological Impact of Ocean Acidification in the Canadian Arctic: Widespread Severe Pteropod Shell Dissolution in Amundsen Gulf

Andrea Niemi^{1*}, Nina Bednaršek^{2,3}, Christine Michel¹, Richard A. Feely⁴, William Williams⁵, Kumiko Azetsu-Scott⁶, Wojciech Walkusz¹ and James D. Reist¹

¹ Fisheries and Oceans Canada, Freshwater Institute, Winnipeg, MB, Canada, ² Southern California Coastal Water Research Project, Costa Mesa, CA, United States, ³ National Institute of Biology, Ljubljana, Slovenia, ⁴ NOAA Pacific Marine Environmental Laboratory, Seattle, WA, United States, ⁵ Fisheries and Oceans Canada, Institute of Ocean Sciences, Sidney, BC, Canada, ⁶ Fisheries and Oceans Canada, Bedford Institute of Oceanography, Dartmouth, NS, Canada

OPEN ACCESS

Edited by:

Xinping Hu,
Texas A&M University Corpus Christi,
United States

Reviewed by:

Elizabeth H. Shadwick,
Oceans and Atmosphere (CSIRO),
Australia
Silke Lischka,
GEOMAR Helmholtz Centre for Ocean
Research Kiel, Germany

*Correspondence:

Andrea Niemi
Andrea.Niemi@dfo-mpo.gc.ca

Specialty section:

This article was submitted to
Marine Biogeochemistry,
a section of the journal
Frontiers in Marine Science

Received: 28 September 2020

Accepted: 19 February 2021

Published: 11 March 2021

Citation:

Niemi A, Bednaršek N, Michel C,
Feely RA, Williams W, Azetsu-Scott K,
Walkusz W and Reist JD (2021)
Biological Impact of Ocean
Acidification in the Canadian Arctic:
Widespread Severe Pteropod Shell
Dissolution in Amundsen Gulf.
Front. Mar. Sci. 8:600184.
doi: 10.3389/fmars.2021.600184

Increasing atmospheric CO₂, cold water temperatures, respiration, and freshwater inputs all contribute to enhanced acidification in Arctic waters. However, ecosystem effects of ocean acidification (derived from anthropogenic and/or natural sources) in the Arctic Ocean are highly uncertain. Zooplankton samples and oceanographic data were collected in August 2012–2014 and again in August 2017 to investigate the pelagic sea snail, *Limacina helicina*, a biological indicator of the presence and potential impact of acidified waters in the Canadian Beaufort Sea. Between 2012 and 2014 *L. helicina* abundance ranged from <1 to 1942 Ind. m⁻², with highest abundances occurring at stations on the Canadian Beaufort Shelf in 2012. The majority of individuals (66%) were located between 25 and 100 m depth, corresponding to upper halocline water of Pacific origin. In both 2014 and 2017, >85% of *L. helicina* assessed (*n* = 134) from the Amundsen Gulf region displayed shell dissolution and advanced levels of dissolution occurred at all stations. The severity of dissolution was not significantly different between 2014 and 2017 despite the presence of larger individuals that are less prone to dissolution, and higher food availability that can provide some physiological benefits in 2014. Corrosive water conditions were not widespread in the Amundsen Gulf at the time of sampling in 2017, and aragonite undersaturation ($\Omega_{ar} < 1$) occurred primarily at depths > 150 m. The majority of dissolution was observed on the first whorl of the shells strongly indicating that damage was initiated during the larval stage of growth in May or early June when sea ice is still present. Evidence of shell modification was present in 2014, likely supported by abundant food availability in 2014 relative to 2017. The proportion of damaged *L. helicina* collected from coastal embayments and offshore stations is higher than in other Arctic and temperate locations indicating that exposure to corrosive waters is spatially widespread in the Amundsen Gulf region, and periods of exposure are extreme enough to impact the majority of the population.

Keywords: arctic, pteropods, *Limacina helicina*, ocean acidification, life history, sea ice

INTRODUCTION

The intrusion of CO₂ into the oceans is supporting the acidification of waters in regions around the Arctic (AMAP, 2018). Reduced summer sea ice provides a positive feedback to CO₂ uptake as ocean-air gas exchange is enhanced by the larger areas and longer periods of open water (Cross et al., 2018; Zhang et al., 2020). Additional factors, including water mass transport, low water temperatures, upwelling, riverine inflow, sea ice meltwater, and respiration, contribute to the acidification process and create regional differences in the extent and duration of low pH waters (Feely et al., 2008, 2016; Azetsu-Scott et al., 2010, 2014; Robbins et al., 2013; Qi et al., 2017). Biological effects of Arctic ocean acidification, derived from anthropogenic and/or natural sources (IPCC, 2011), are highly uncertain at individual to ecosystem scales.

With increasing acidity, the saturation state of calcium carbonate (CaCO₃) minerals (e.g., aragonite, calcite) decreases creating suboptimal conditions for the formation and maintenance of shells. The CaCO₃ saturation state (Ω) is the product of calcium and carbonate ion concentrations divided by the apparent stoichiometric solubility product for either aragonite or calcite (Feely et al., 2008). The calcium ion concentration is estimated from the salinity, and the carbonate ion concentration is calculated from measurements of the dissolved inorganic carbon (DIC) and total alkalinity (TA). With increased exposure to undersaturated conditions, physical damage (e.g., shell dissolution) as well as physiological costs, may impact feeding, growth or reproduction (Kroeker et al., 2013; Bednaršek et al., 2017a) of a variety of benthic and pelagic calcifying species and fish of high-latitude habitats, such as red king and Tanner crabs (Long et al., 2013), bivalves (Klok et al., 2014), and salmon (Ou et al., 2015; Williams et al., 2019).

The planktonic sea snail, *Limacina helicina*, is the most common shelled pteropod in arctic waters. This genus is found in all oceans, and is particularly abundant at high-latitudes (Bednaršek et al., 2012a). It produces an external aragonite shell (Bednaršek et al., 2012a). Aragonite is a metastable polymorph of calcium carbonate that is 1.5 times more soluble in seawater than are shells secreted from calcite (Fabry et al., 2008). Consequently, *L. helicina* is sensitive to dissolution under corrosive conditions and is a sensitive indicator of the presence and impacts of acidified water. In corrosive waters ($\Omega_{ar} < 1 \sim 1.5$ for pteropods; Bednaršek et al., 2019), *L. helicina* can be affected by varying degrees of shell dissolution (Bednaršek et al., 2012b) with concurrent declines in calcification (Comeau et al., 2010), decreases in growth (Lischka et al., 2011; Gardner et al., 2018) and, increased mortality (Busch et al., 2014; Bednaršek et al., 2017a).

Limacina helicina is known to occur on the Canadian Beaufort Shelf and in the Amundsen Gulf during the open-water period (Darnis et al., 2008; Walkusz et al., 2013). In this study *L. helicina* was selected as a biological indicator of ocean acidification in the Canadian Beaufort Sea. This region has relatively low Ω_{ar} compared to other ocean regions due to colder water temperatures and regional circulation patterns, especially the inflow of naturally corrosive, undersaturated Pacific halocline

waters (Fabry et al., 2009; Mathis et al., 2015; Qi et al., 2017; Cross et al., 2018; Mol et al., 2018). Reductions in saturation state of halocline waters is occurring off (i.e., Canada Basin) and on the shelf (i.e., upper halocline) (Miller et al., 2014; Qi et al., 2017; AMAP, 2018; Cross et al., 2018; Mol et al., 2018) and increases in upwelling are expected to enhance localized and periodic undersaturation events as the halocline waters mix with and displace supersaturated surface waters (Mathis et al., 2012, 2015; Qi et al., 2017; Mol et al., 2018).

Given the current state of ocean acidification in Arctic waters, and expected declines in aragonite saturation, the objectives of this study were to, (1) identify the distribution of *L. helicina*, in offshore habitats of the Canadian Beaufort Sea and in coastal embayments of the Amundsen Gulf not previously assessed and, (2) evaluate the presence and extent of *L. helicina* shell dissolution in years with contrasting sea-ice opening (2014 and 2017) to identify potential environmental drivers of the observed dissolution. Earlier opening of the sea ice could affect multiple factors relevant to pteropod status including mixing of saturated and undersaturated waters, as well changes in the timing and availability of food. This study provides an initial assessment of the biological impact of acidified waters in the Canadian Beaufort Sea, comparing effects among different habitats of the Amundsen Gulf. We hypothesized that highest shell dissolution would be associated with areas of known upwelling, specifically Cape Bathurst and Cape Parry in the Anguniaqvia niqiqyuam Marine Protected Area, because of exposure to low Ω_{ar} .

MATERIALS AND METHODS

Study Area

Sampling locations varied between years due to sea-ice conditions and program priorities. Sampling on the Canadian Beaufort Shelf extended to slope waters in 2012 and to the west side of Banks Island in 2014 (Figure 1). In the Amundsen Gulf, sampling extended eastward to Dolphin and Union Strait and five different embayments were sampled (Franklin, Darnley, Wise and Walker bays, and Minto Inlet). Water depth in embayments (i.e., Minto Inlet and Franklin Bay) approaches 300 m in deep channels whereas water depth reaches over 600 m in the central basin of the Amundsen Gulf (Figure 1). The water column of the study area is stratified and dominated by three main layers depending on station location. Generally, at the time of the study, the nutrient-depleted surface Polar mixed layer (Salinity < 31.6; ca. 0–50 m depth) lays over the nutrient rich Pacific halocline (32.4 < Salinity > 33.1; ca. 50–200 m), and the warm Atlantic layer (Salinity > 34) is located at depths >200 m (Carmack and MacDonald, 2002). The water layers are influenced by dynamic physical oceanographic processes including cross-shelf and localized upwelling and eddies (Williams and Carmack, 2008; Sévigny et al., 2015; Kirillov et al., 2016) as well as seasonally variable inflow of the Mackenzie River.

Shell dissolution results are compared among three areas (Figure 1) with different oceanographic conditions, (1) the recurrent upwelling areas of Cape Bathurst (CPB transect) and Cape Parry (CPY transect), (2) Dolphin and Union Strait (DOL

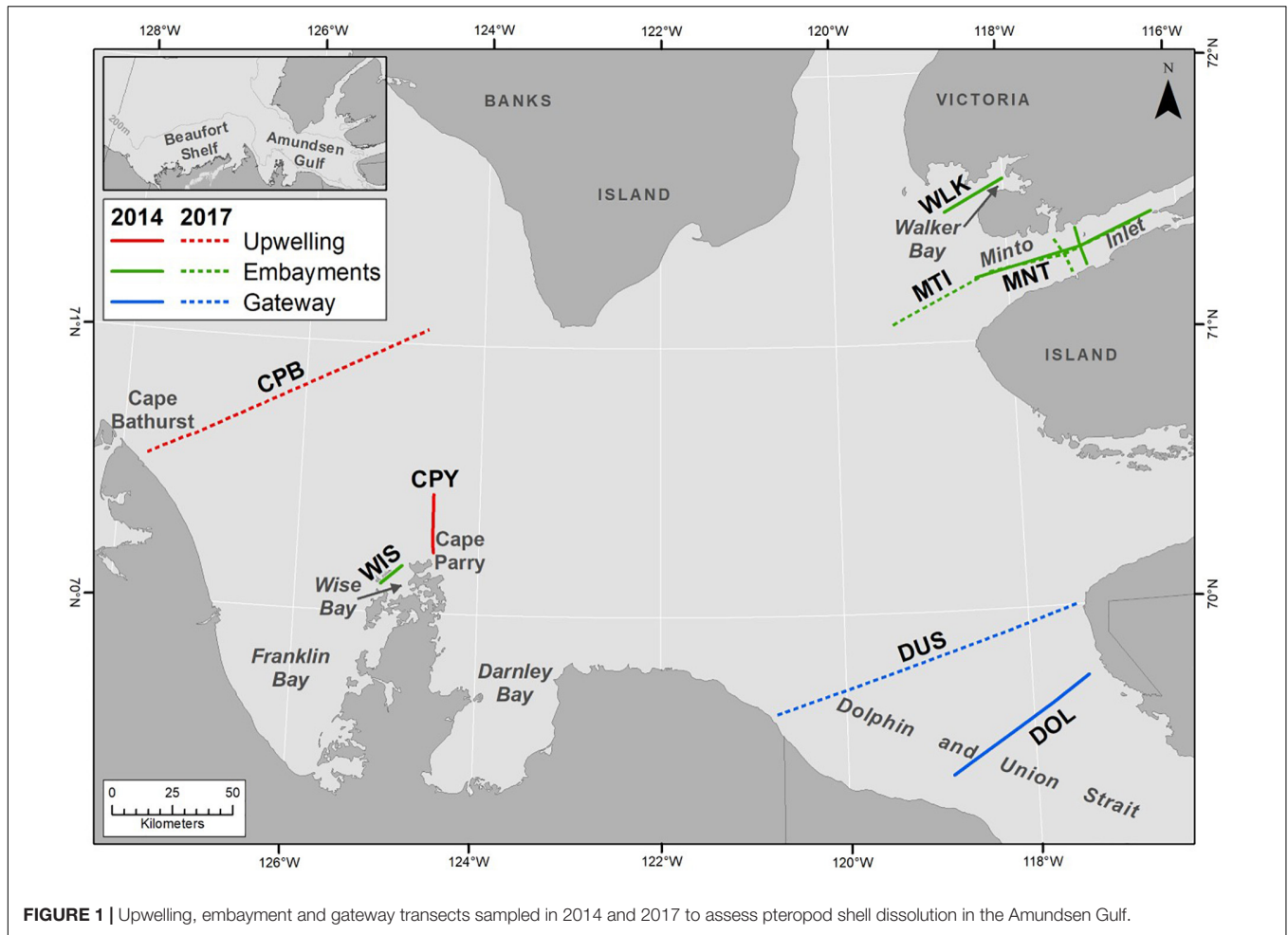


FIGURE 1 | Upwelling, embayment and gateway transects sampled in 2014 and 2017 to assess pteropod shell dissolution in the Amundsen Gulf.

and DUS transects), an oceanographic gateway between the Amundsen Gulf and the Coronation Gulf of the Kitikmeot region, and, (3) small embayments of Amundsen Gulf (Wise (WIS transect) and Walker Bay (WLK transect), and Minto Inlet (MNT and MTI transects) that have a semi-distinct circulation relative to the central gulf. During the ice-covered period, the upwelling and gateway areas are generally covered with seasonal pack ice whereas the small embayments are covered with seasonal land-fast ice.

Sampling and Analyses

From 2012 to 2014 sampling was conducted as part of the Beaufort Regional Environmental Assessment Marine Fishes program (BREA-MFP) and in 2017 work continued as part of the Canadian Beaufort Sea-Marine Ecosystem Assessment (CBS-MEA) program. In all years sampling occurred between the first week of August and mid-September. During this period there is no polar night (complete darkness). Twilight illumination increases at the end of August with daylight decreasing to ca. 13 h by mid-September.

Zooplankton sampling and CTD casts were conducted in all years along transects that ranged in depth from 20 m to a maximum of 1020 m on the lower slope of the Beaufort Shelf. At

each station, physical oceanographic data (salinity, temperature, and dissolved oxygen) were collected with a rosette-mounted Seabird SBE-25 CTD and averaged over 1 m intervals. Herein we provide chlorophyll *a* (chl *a*) concentrations from 2014 to 2017, corresponding to the years of shell dissolution analyses. Total chl *a* was determined from discrete water samples collected with the rosette. Duplicate chl *a* subsamples were filtered onto 25-mm Whatman GF/F filters and extracted for 24 h in 90% acetone at 4°C in the dark, for fluorometric determination (10AU Turner Designs fluorometer), according to Parsons et al. (1984).

Sampling for DIC and TA occurred in 2017 only. DIC and TA samples were collected from the rosette in 250 ml borosilicate glass bottles and preserved with mercuric chloride following the best practices (Dickson et al., 2007). The DIC was determined using gas extraction and a coulometric titration with photometric endpoint detection (Johnson et al., 1985). The TA was measured by open-cell potentiometric titration with a full curve Gran endpoint determination (Haradsson et al., 1997). All measurements were calibrated using Certified Reference Material supplied by A. Dickson, Scripps Institute of Oceanography. Precision of measurements for DIC and TA was better than 0.1 and 0.2%, respectively. The saturation state of seawater with respect to aragonite was calculated from the DIC and TA measurements

with the CO2SYS program (Lewis and Wallace, 1998) using the dissociation constants of Lueker et al. (2000) and the boron constant of Lee et al. (2010).

The vertical distribution of *L. helicina* was determined from zooplankton taxonomy samples (2012–2014, 2017) collected with a HYDRO-BIOS MultiNet, type Midi (0.25 m² aperture, 150 μm mesh) deployed to within 10 m of the bottom. All zooplankton sampling was conducted during the daytime hours, ca. 7 am to 6 pm local time. The net was hauled vertically and programmed to collect stratified samples from a maximum of five depth strata. Targeted strata were generally 0–25 m, 25–50 m, 50–100 m, 100–200 m, and >200 m. Samples from each depth stratum were preserved in a 4% buffered formaldehyde solution in seawater. Samples processed in the lab were split using a Folsom splitter (2012, Fisheries and Oceans Canada, Freshwater Institute) or beaker method (2013, 2014, Van Guelpen et al., 1982, Huntsman Marine Institute). *L. helicina* was identified from splits containing ca. 300 individuals or from larger fractions when rare. From the 2017 CBS-MEA zooplankton samples, only select stations from CPB, MTI and DUS transects were analyzed to inform the three oceanographic areas identified for shell dissolution comparisons (Figure 1). Abundances presented as Ind. m⁻² have been integrated over the entire water column, to the maximum sampling depth at each station.

In 2014 and 2017, *L. helicina* was opportunistically collected from MultiNet or oblique Bongo net (500 μm mesh) tows at stations within the three focal areas. Individual specimens were carefully picked, without magnification, from fresh samples for dissolution analyses. The individual *L. helicina* were rinsed with fresh water to remove salts and stored frozen at –80°C until analysis. Such preservation eliminated any potential of shell dissolution during the storage.

Limacina helicina shell dissolution was assessed by scanning electron microscopy (SEM). Shells were prepared for SEM analysis by, (i) removal of abiogenic crystals from the shell surface, (ii) dehydration, (iii) mounting on the SEM stub, (iv) removal of the organic layer, and (v) sputter coating. Detailed procedures are provided in Bednaršek et al. (2012b), noting that a longer period (ca. 25 min versus 15–20 min) was needed to remove the organic layer from the larger individuals collected in the Amundsen Gulf. SEM images of shell microstructure were taken across the entire shell and a stage of dissolution [no dissolution, Type I, II, or III (Table 1)] was assigned to each individual based on the extent of pitting, cracks, and/or areas where aragonite crystals were absent, porous or dissolved. Shell size and the distribution of shell damage were recorded. Descriptions of each dissolution category and associated saturation condition from other studies are summarized in Table 1.

RESULTS

Environmental Conditions

There was at most a 1-month time difference in the start of sea-ice opening during the years when shell dissolution was assessed (2014 and 2017). In 2014 the day of sea-ice opening

[DOO, last day sea-ice concentration drops below 80% before the first summer minimum (Peng et al., 2018); data from the Canadian Ice Service] occurred during the week following June 2nd and July 7th at Cape Bathurst and Minto Inlet, respectively. In 2017 the DOO was earlier relative to 2014, occurring during the week following May 8th and June 26th at the same respective locations. The sea-ice loss period occurs over a period of weeks in the Dolphin and Union Strait area, with bands of fractured ice persisting in the area. In contrast to Cape Bathurst and Minto Inlet, the DOO was slighter earlier in 2014 relative to 2017, estimated for the week following May 19 and May 29, respectively.

The water masses in Amundsen Gulf, that set the general physical and geochemical conditions, mostly originate from outside the gulf. The three dominant water masses (polar mixed layer, Pacific halocline and Atlantic layer) were present in each of the three areas where shell dissolution was assessed, and the water column structure was generally similar in 2014 and 2017 (Figure 2). Deeper waters flow in to the gulf, and extend into the embayments, from the Beaufort continental slope, and from the offshore Beaufort Gyre. The Atlantic-origin bottom waters transitioned to Pacific-origin water (Figure 2) around 200 m depth. The Pacific-origin waters included Pacific Winter Water, identified by the temperature minimum (~–1.3°C) at ~150 m deep (see Figure 2 at salinity ~33), and Pacific Summer Water, identified by the temperature maximum (~–0.2°C) at ~50 m deep (see Figure 2 at salinity ~31).

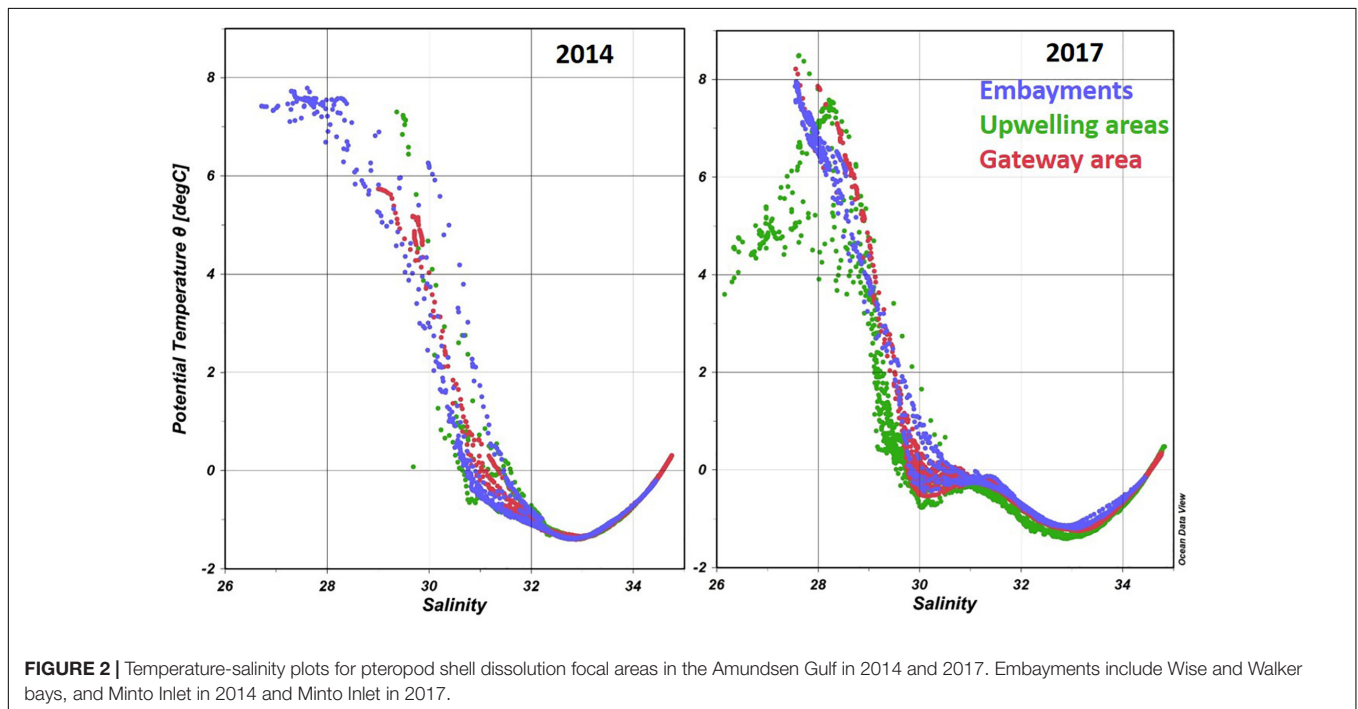
As is expected for the Arctic Ocean, surface waters in the three areas were generally freshened due to a combination of factors including river water input, ice melt, and the advection and mixing of lower salinity waters. In the Amundsen Gulf, the direct river inputs are from the relatively small rivers, such as the Hornaday River that flows into Darnley Bay. The large inflow from the Mackenzie River can also have a direct influence when summertime downwelling favorable winds occur on the shelf, pushing Mackenzie River water to the coast where it rapidly flows into the Amundsen Gulf in a boundary current. In 2017 surface water freshening is especially evident at Cape Bathurst (salinity as low as 26) where Mackenzie River plume waters are more frequently observed.

In 2017, aragonite saturation in the Amundsen Gulf ranged from 0.95 to 3.43 (average 1.47) in the surface mixed layer (0–50 m), 0.69–2.15 (average 1.09) in the Pacific halocline (50–200 m), and 0.72–1.40 (average 1.10) in waters deeper than 200 m (Figure 3), similar to summer measurements in Shadwick et al. (2011). Aragonite undersaturation occurred at upwelling, embayment and gateway stations, with 98% of undersaturated samples occurring between 100 and 600 m. Aragonite saturation state, over the entire water column, was correlated to dissolved oxygen concentrations at Cape Bathurst, Minto Inlet, and Dolphin and Union Strait ($r = 0.50$, $p < 0.01$).

Chlorophyll *a* integrated concentrations over the euphotic zone were, on average, four times higher in 2014 than 2017 at the stations in the Amundsen Gulf. In the three areas assessed for dissolution, integrated euphotic zone (maximum 100 m depth) chl *a* concentrations averaged 54.1 ± 35.5 mg m⁻² and 14.1 ± 2.2 mg m⁻² in 2014 and 2017, respectively. In 2014,

TABLE 1 | Descriptive features of pteropod shell dissolution stages and associated saturation conditions as described in Bednaršek et al. (2012b).

Dissolution Type	Shell Dissolution Features	Saturation Conditions
Type I	<ul style="list-style-type: none"> • First indices of slightly increased porosity • Aragonite crystals within the upper-prismatic layer affected by dissolution. ‘Cauliflower heads’ present 	<ul style="list-style-type: none"> • In a small extent present in the natural environment • Widespread at decreased Ω_{ar} supersaturation
Type II	<ul style="list-style-type: none"> • Increased porosity • Dissolved patches more extensive and numerous • Prismatic layer partially or completely dissolved; crossed-lamellar layer exposed 	<ul style="list-style-type: none"> • In small extent present at transitional saturation states; more common in undersaturated conditions
Type III	<ul style="list-style-type: none"> • Less compact crystal structure with compromised shell integrity and extreme frailness • Dissolution within crossed-lamellar layer with crystals thicker and chunkier 	<ul style="list-style-type: none"> • At transitional Ω_{ar} conditions; larger, more extensive patches in Ω_{ar} undersaturated conditions, particularly with increased time of exposure

**FIGURE 2** | Temperature-salinity plots for pteropod shell dissolution focal areas in the Amundsen Gulf in 2014 and 2017. Embayments include Wise and Walker bays, and Minto Inlet in 2014 and Minto Inlet in 2017.

the highest chl *a* concentrations occurred in the embayments, reaching 144.5 mg m^{-2} in Wise Bay. Primary production contributed to the observed Ω_{ar} supersaturation in the surface waters at the time of sampling and given that maximum values of Ω_{ar} correspond with peak summer open-water phytoplankton concentrations in Amundsen Gulf (Shadwick et al., 2013), it is expected that euphotic zone Ω_{ar} would have been higher in August/September 2014 than measured in August/September 2017 (Figure 3).

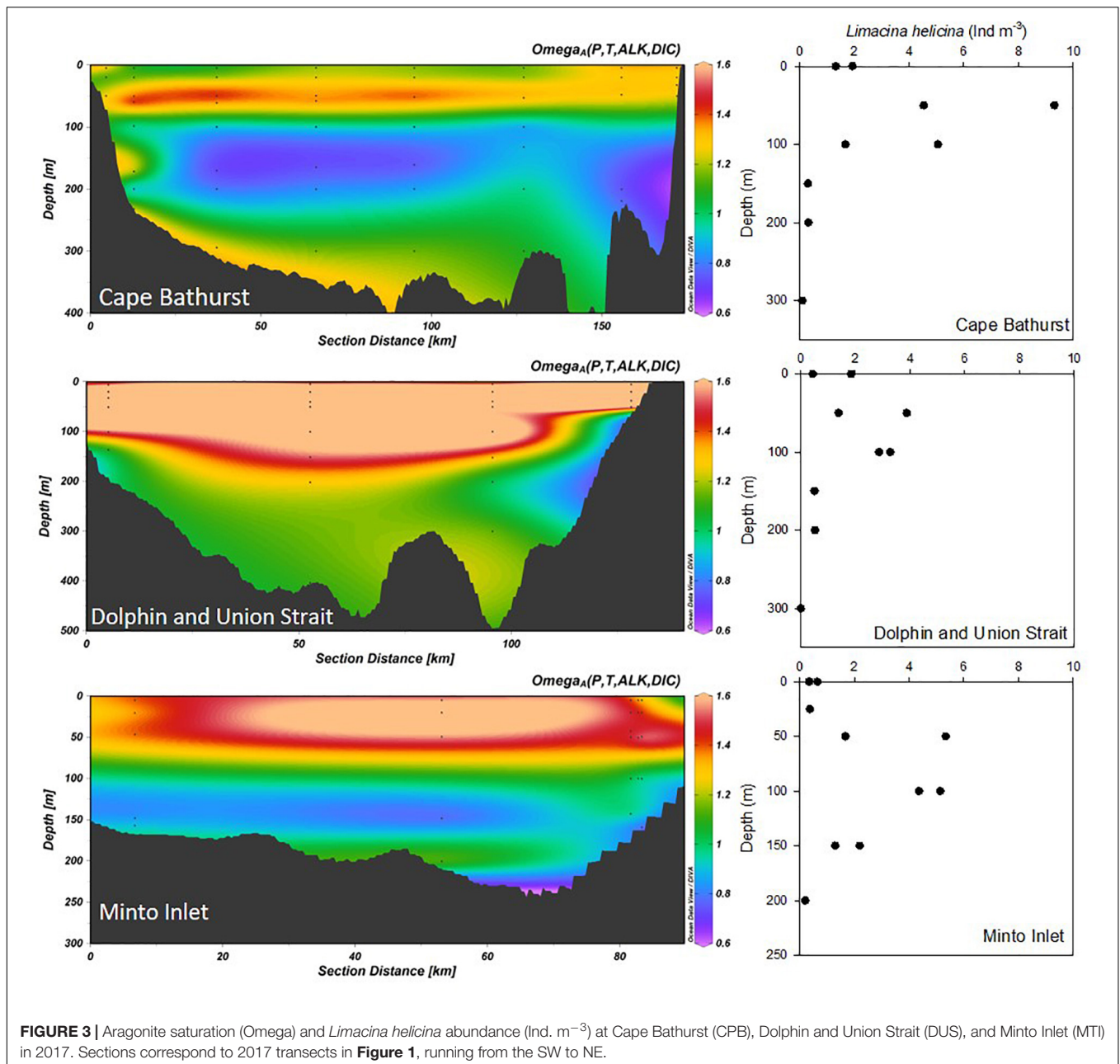
***Limacina helicina* Distribution**

The abundance and distribution of *L. helicina* varied spatially and between years (2012–2014) on the Beaufort Shelf and in the Amundsen Gulf (Figure 4). These pteropods were found in all small embayments, i.e., Wise and Walker bays and Minto Inlet, sampled for the first time, indicating that this species is widely distributed in near-shore as well as offshore areas of the Canadian Beaufort Sea. Shelf waters contained the

highest number of individuals in 2012 (water column integrated abundance, maximum 1942 Ind. m^{-2}). However, they were not found or occurred at abundances $\leq 5 \text{ Ind. m}^{-2}$ during repeat sampling on the shelf in 2014. In the Amundsen Gulf, *L. helicina* was found primarily in surface waters (86% of individuals in 0–25 m strata) of offshore stations in 2013, whereas they were more broadly distributed in 2014 (Figure 4). In 2017, *L. helicina* abundance ranged from 0 to 625 Ind. m^{-2} at select stations from the Cape Bathurst, Minto Inlet and Dolphin and Union Strait transects (Figure 3), with the majority of individuals distributed between the 50–100 m ($52 \pm 35\%$) and the 100–200 m ($32 \pm 22\%$) depth strata. The abundance of *L. helicina* in 2017 was not correlated to Ω_{ar} but was weakly correlated to dissolved oxygen concentrations (Kendall's $\tau = 0.37$, $p = 0.01$).

Shell Size and Growth Pattern

The diameter of individuals assessed for shell dissolution averaged $932.2 \pm 469.8 \text{ }\mu\text{m}$ in 2014 and $732.1 \pm 357.7 \text{ }\mu\text{m}$



in 2017. There was no significant difference in the size of individuals collected in August versus September suggesting limited growth during the study period (**Figure 5**). Among the individuals assessed for shell dissolution, there were two size classes present. Firstly, the majority of individuals was between 500 and 700 μm in size and can be considered juveniles, and secondly, adult individuals $\geq 1000 \mu\text{m}$ that were present in small numbers compared to the juveniles. The low numbers of adults present (<10% of examined individuals) during the August to September sampling period in 2014 and 2017, indicates that the peak of adults was probably earlier in the spring with spawning occurring in May–June, just prior to or at the time of sea-ice melt/break-up. A May/June spawning is consistent with larvae

developing into the juveniles that were found in the August–September period.

Shell Dissolution

In both years, every individual assessed displayed some level of shell dissolution indicative of decreased supersaturation or undersaturated Ω_{ar} conditions. Levels of dissolution (**Table 1**) were similar in 2014 (Type I 17%, Type II 13%, Type III 70%) and 2017 (Type I 10.5%, Type II 18.5%, Type III 71%) (**Figure 6**). There were no individuals detected without shell dissolution but the shells were not entirely covered with dissolution damage; rather spots of the various Type I–III dissolutions were observed in discrete locations on the shells

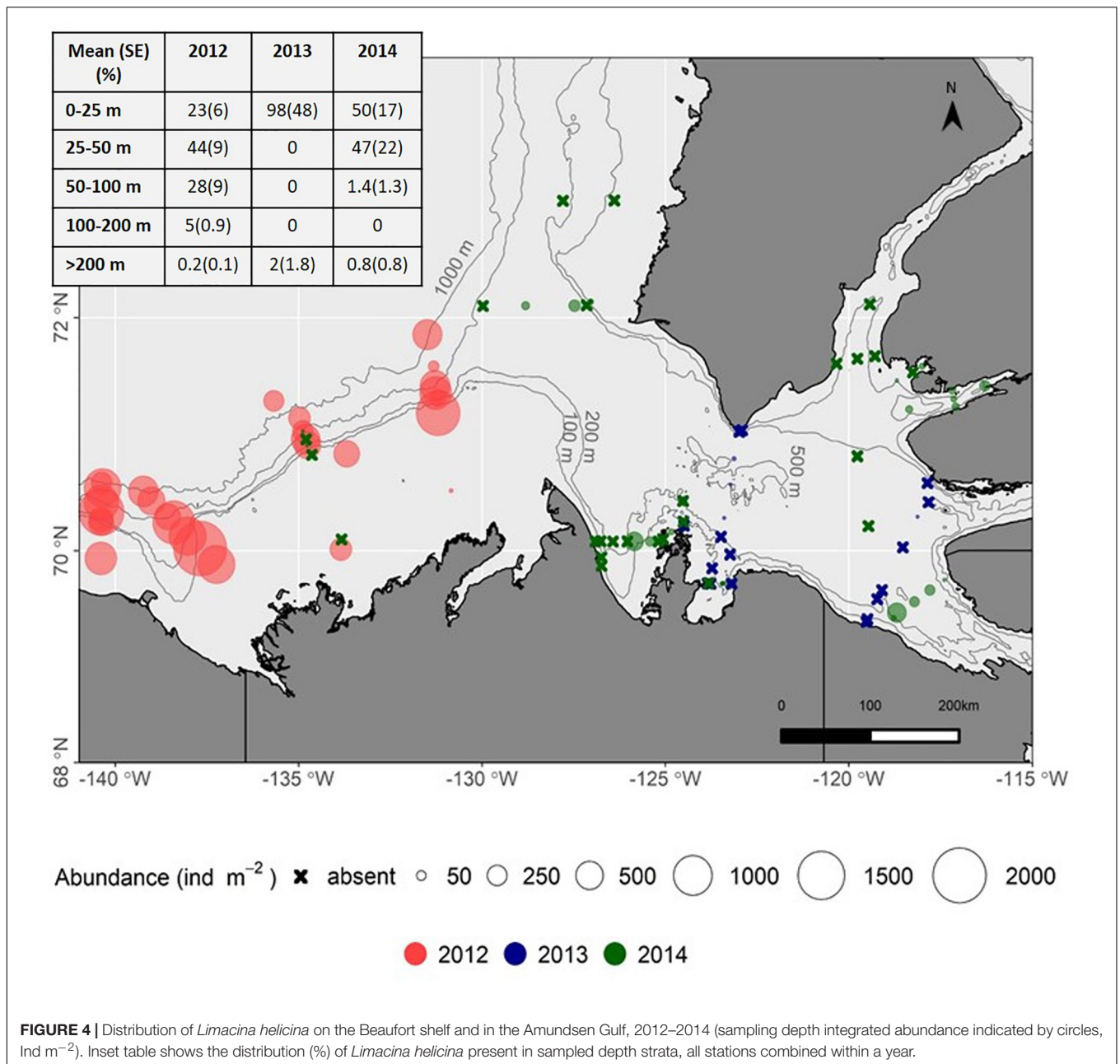
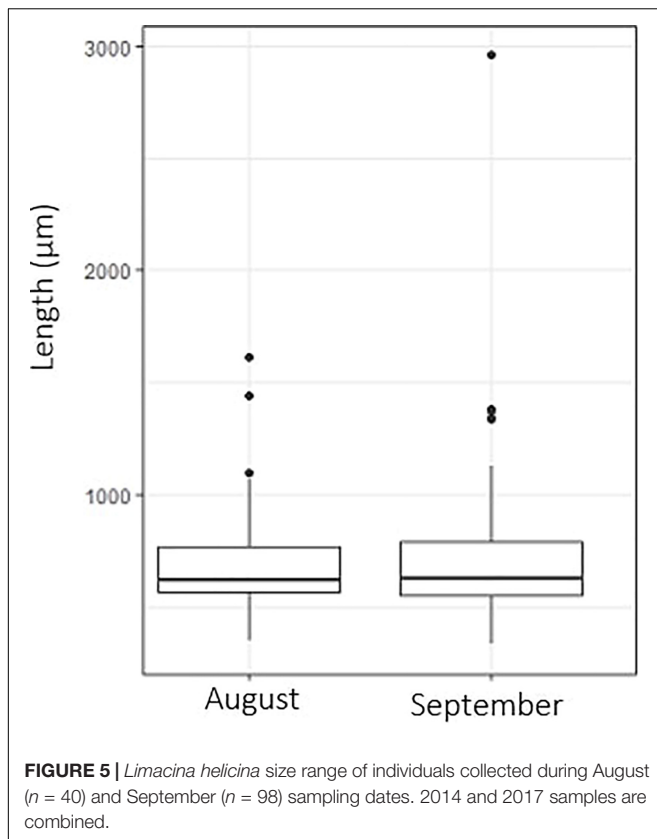


(Figure 7). The high percentage of Type III dissolution indicates a very high incidence of the most severe dissolution present. The ratio of shells with dissolution linked to undersaturated ($\Omega_{ar} < 1$) conditions (i.e., Type II + Type III) was not significantly different between years (Wilcoxon, $p = 0.4$) and the extent of shell dissolution did not significantly vary between the upwelling ($n = 41$), embayment ($n = 60$), or Dolphin and Union Strait gateway ($n = 33$) areas (Kruskal-Wallis, $p = 0.4$ – 0.7 ; Figure 8). The ratio of individuals with Type II or Type III dissolution was not significantly correlated to Ω_{ar} measured at the time of sampling but the occurrence of Type II and Type III dissolution did increase with increasing average salinity (Kendall's $\tau = 0.40$, $p = 0.02$).

Higher average salinity was found in the Pacific and Atlantic layers, relative to the surface polar mixed layer, corresponding to the seasonal occurrence of undersaturated Ω_{ar} conditions in the deeper layers.

For the 2014 sampling period, the majority of the most intense shell dissolution (Type III) occurred in Walker Bay (93% of individuals) followed by similar dissolution rates in Minto Inlet (80% of individuals) and Dolphin and Union Strait (83% of individuals), whereas only 40% of individuals from Cape Parry showed Type III dissolution. In 2014 the most severe dissolution occurred for samples collected between 25 and 80 m depth, and several individuals from Minto Inlet and Dolphin and Union Strait, collected from > 150 m, also exhibited Type III dissolution.



In 2017 the highest occurrence of Type III dissolution (93% of individuals) was found at stations along the Cape Bathurst transect, followed by Dolphin and Union Strait (63% of individuals) and Minto Inlet (70% individuals) stations. General trends for Type II and Type III dissolution seem to indicate more dissolved shells in the inlets/nearshore areas, with a gradual decrease in dissolution intensity with increasing distance from shore. Similar to 2014, water depths ca. 25–50 m had the highest occurrence of Type II and Type III dissolution although stations along the Dolphin and Union Strait transect had the majority (12 of 18 individuals) of Type III dissolution at depths > 100 m.

Distribution of Shell Dissolution

The most significant extent of shell dissolution damage occurred on the first whorl (Figure 7) across stations and individuals, although smaller extents of dissolution were also scattered around the shell, in particular at the growing edge. The extent of overall shell dissolution is likely linked to the various degrees of Ω_{ar} throughout the pteropod life history, with the growing edge dissolution linked to the most recent $\Omega_{ar} < 1$ conditions. The most intense shell dissolution on the first whorl most likely relates to when Ω_{ar} conditions were lower during the period of sea-ice melt when early life stages were present. Given that the timing of sea-ice melt likely coincides with the spawning event, the low Ω_{ar} conditions at the time of spawning would explain the most extensive dissolution on the larval shell around the first whorl.

In 2014 there was evidence of shell structural modification in the adults, but not in juveniles (Figure 9). Shell modification was focused around the first whorl, and was evident as a crystalline regrowth overlaid on surface areas of dissolution. This structural modification in the shape of crystalline regrowth was unstructured and homogenous, and in this, distinctively different than the typical prismatic and underlying cross-lamellar microstructure of pteropod shells (Sato-Okoshi et al., 2010). Shell modification was evident on few individuals, in particular where the shell dissolution was most severe, and not across all the adults. In 2017, there was no or extremely limited evidence of shell modification, again only in the adult group, indicating some plastic responses in adults, but not in the juveniles.

DISCUSSION

Abundance and Growth of the Pteropod *Limacina helicina*

Limacina helicina was widely distributed across the study area including coastal embayments. Although the occurrence of dissolution was severe and consistent in 2014 and 2017, *L. helicina* abundance was variable between years (Figure 4). Highest abundance was observed on the Beaufort shelf (1948 Ind. m^{-2}) within the range previously observed during cross-shelf transects in the same region (0 to >10,000 Ind. m^{-2} , Walkusz et al., 2010; Smoot and Hopcroft, 2017). Abundances measured in the Amundsen Gulf were similar to later season (September/October) sampling reported by Darnis et al. (2008). Abundances recorded on the Beaufort shelf are among the highest recorded since the 1950s (Bednaršek et al., 2012a), identifying the Beaufort Sea as an important pteropod hotspot across all ocean regions. Despite the sensitivity of polar waters to ocean acidification, dense populations of *Limacina* spp. also occur in Antarctic waters (e.g., Bednaršek et al., 2012c; Nishizawa et al., 2016) and it is evident that *L. helicina* life history is well adapted to the short productive season on Arctic shelves.

Limacina helicina abundance was not correlated with aragonite saturation (Ω_{ar}) at the time of sampling in 2017, and further comparative studies are needed to adequately assess population level responses to annual acidification conditions in the Beaufort Sea. Hypoxia or oxygen minimum zones (dissolved oxygen < 3.5 $ml\ l^{-1}$) have not been detected in the study area suggesting that the positive correlation between *L. helicina* abundance and dissolved oxygen may be a result of food web linkages between zooplankton and primary producers. During the study period, *L. helicina* was distributed primarily in the upper 50 m of the water column (Figure 4) where a subsurface chl *a* maximum is usually located shortly after ice break up, and persists at lower concentrations under post-bloom conditions (Martin et al., 2010). Chlorophyll *a* integrated concentrations over the euphotic zone were, on average, four-times higher in 2014 than 2017 at the stations in the Amundsen Gulf. Oceanographic and sea-ice conditions, and shelf upwelling can drive interannual variations in primary production of this order of magnitude in the Canadian Beaufort Sea, with cascading impacts on

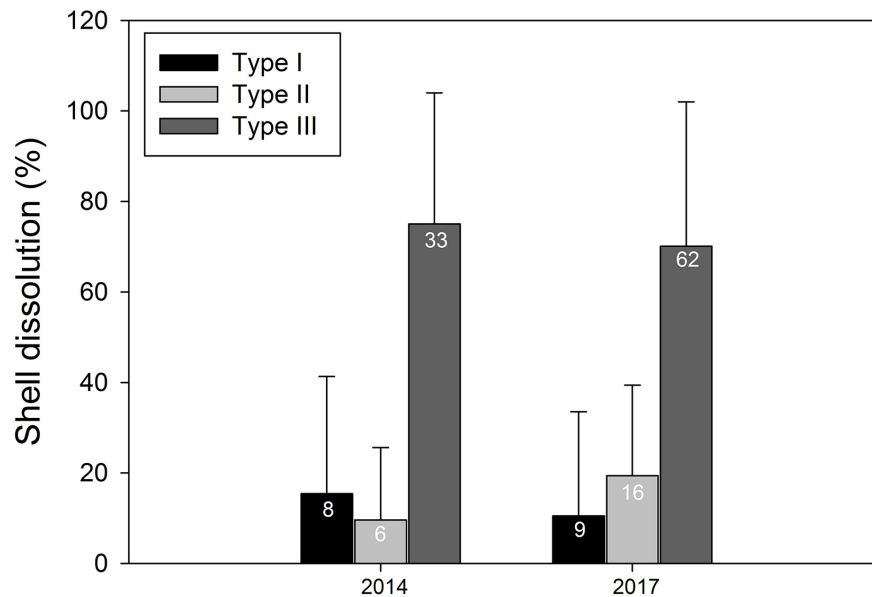


FIGURE 6 | *Limacina helicina* dissolution severity in 2014 and 2017. Sample size (n) indicated on each bar.

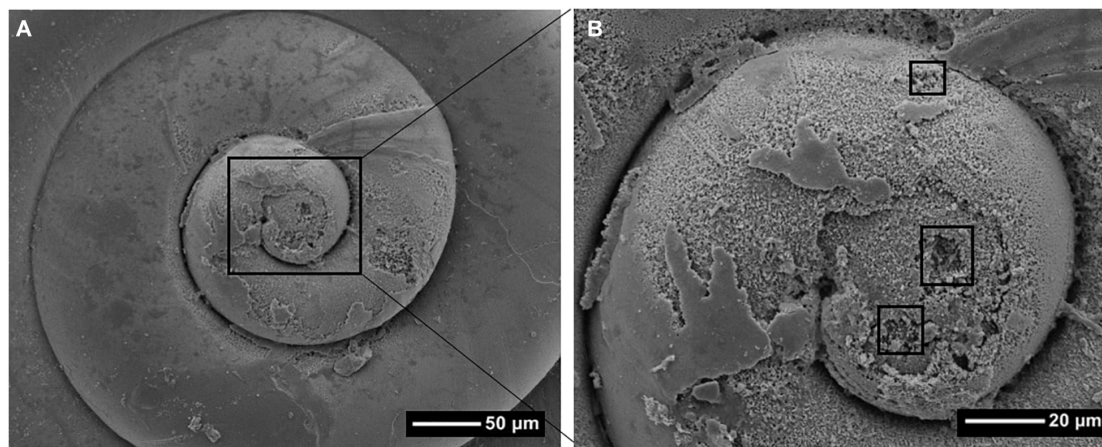


FIGURE 7 | Scanning Electron Microscope (SEM) image **(A)** showing the distribution of dissolution on a *Limacina helicina* shell collected near Cape Bathurst in 2017. In panel **(B)**, damage on the first whorl is shown in greater detail with the squares indicating deeper-protruding Type III dissolution.

food availability to zooplankton grazers (Tremblay et al., 2011). Despite the higher summer chl *a* concentrations in 2014, *L. helicina* abundance was ca. four times lower in 2014 than the 2017 stations assessed (Figure 3). However, individuals were on average larger in 2014 suggesting that the additional summer resources supported enhanced growth but the later ice opening in 2014 may have impeded recruitment, possibly due to a timing mismatch between critical life stages and needed resources.

Growth estimates suggest that *L. helicina* in Amundsen Gulf likely spawned in May or June, coinciding with the sea-ice algal bloom (Riedel et al., 2008; Róžańska et al., 2009) and possible onset of an under-ice or ice-edge phytoplankton bloom in June (Mundy et al., 2009), or early phytoplankton bloom as observed in years of early sea ice retreat (Sallon et al.,

2011). The sea-ice algal bloom provides abundant and critical food (Michel et al., 1996; Kohlbach et al., 2016) to support high growth rates following spawning in surface waters. The consumption of ice algae specifically by pteropods has been identified through food web studies in the high Arctic and in Antarctica (Kohlbach et al., 2016, 2018). Pteropods are reported to feed opportunistically, switching from phytoplankton to mobile prey post-bloom (Gilmer and Harbison, 1991; Pasternak et al., 2017). Open-water isotopic signatures of *L. helicina* from the Beaufort Shelf and Amundsen Gulf indicate pelagic feeding closely linked to phytoplankton ($\delta^{13}\text{C}$ -25.5 ± 0.79 ‰, $\delta^{15}\text{N}$ 9.09 ± 0.8 ‰; Stasko et al., 2017; A. Ehrman unpublished data), in agreement with evidence of an efficient transfer from primary producers to pelagic grazers in this region (Forest et al., 2011; Sallon et al., 2011). Around Cape

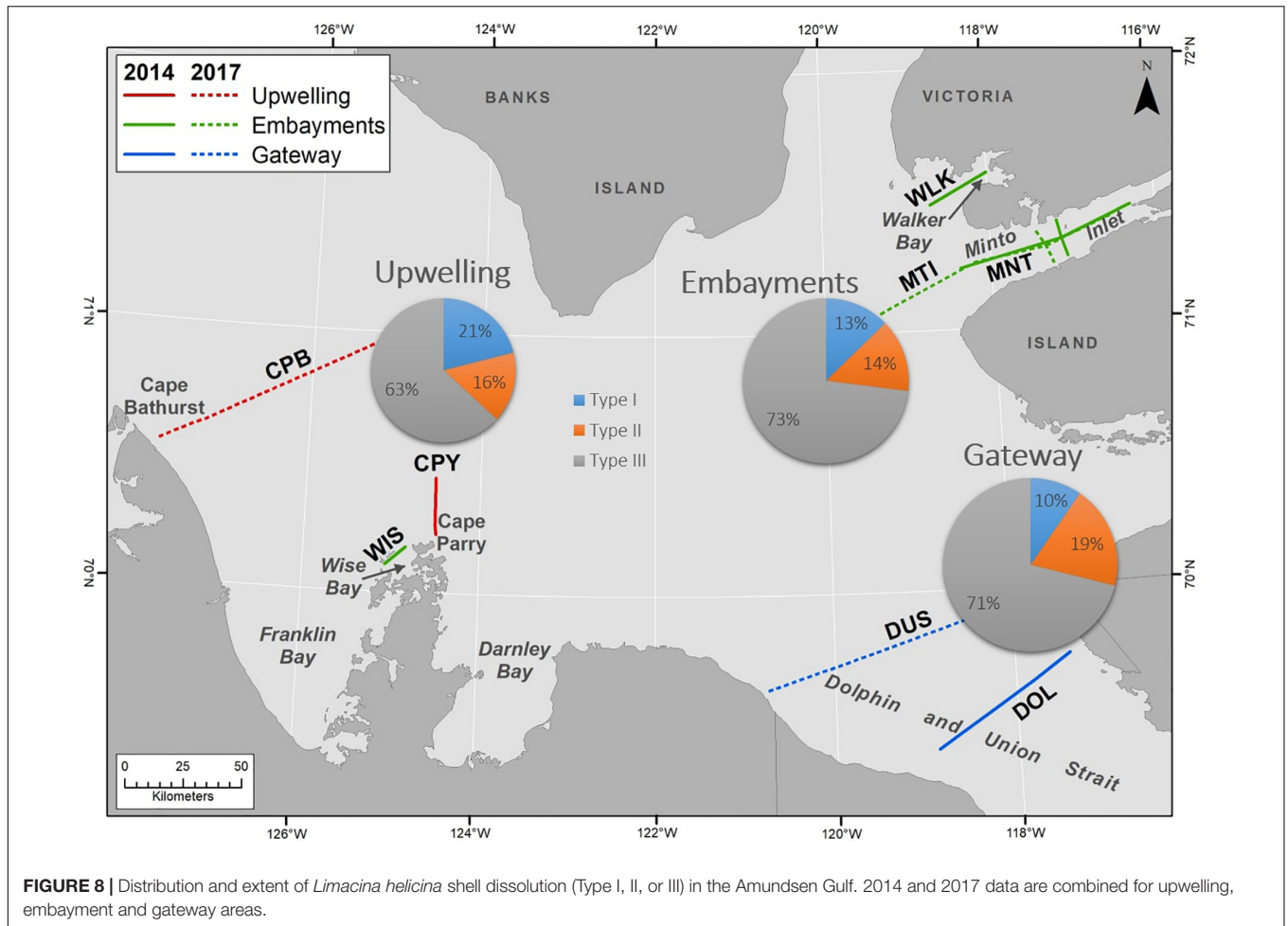


FIGURE 8 | Distribution and extent of *Limacina helicina* shell dissolution (Type I, II, or III) in the Amundsen Gulf. 2014 and 2017 data are combined for upwelling, embayment and gateway areas.

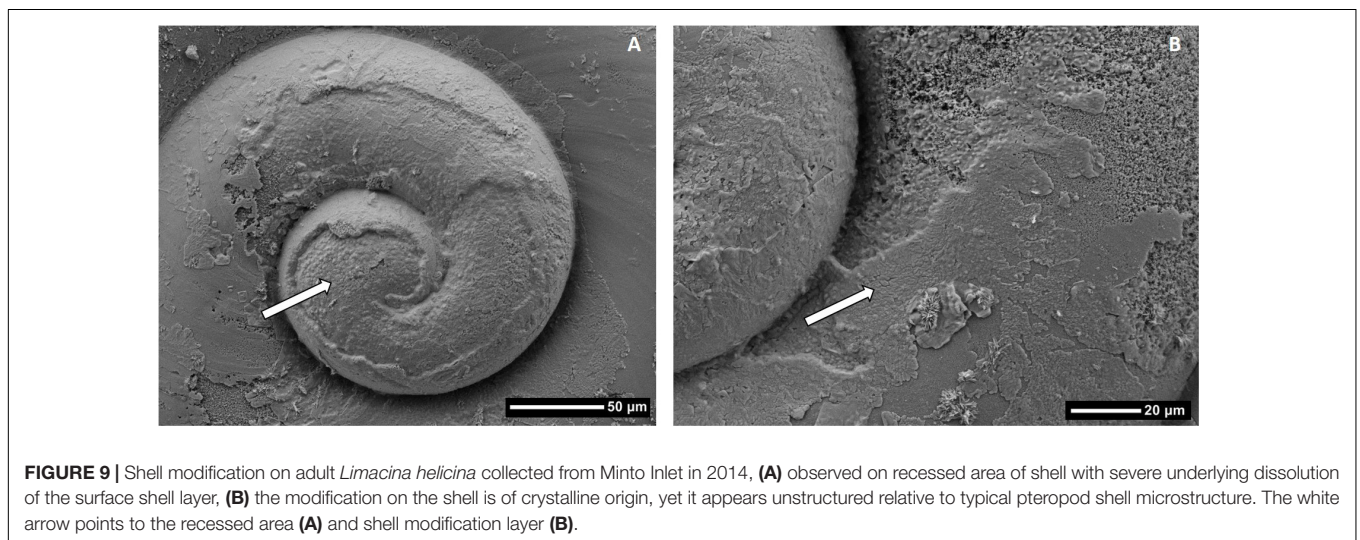


FIGURE 9 | Shell modification on adult *Limacina helicina* collected from Minto Inlet in 2014, (A) observed on recessed area of shell with severe underlying dissolution of the surface shell layer, (B) the modification on the shell is of crystalline origin, yet it appears unstructured relative to typical pteropod shell microstructure. The white arrow points to the recessed area (A) and shell modification layer (B).

Parry, *L. helicina* was trophically positioned more closely to phytoplankton than the key zooplankton grazer, *Calanus hyperboreus* (Niemi et al., 2020). It is likely that herbivory provides the highest quality diet to support *L. helicina* energy

requirements and consequently, tolerance to less favorable ($\Omega_{ar} < 1$) conditions.

The low number and size of adults observed in August indicates a potential mass adult mortality event after spring

spawning. In the study years, the population may have been comprised of a single cohort that overwinters and has a longevity of a single year. The life span of *L. helicina* is location dependent and has been reported to range from one to over 3 years (Kobayashi, 1974; Gannefors et al., 2005; Bednaršek et al., 2012c; Wang et al., 2017). Reliance on the sea-ice algal and spring phytoplankton blooms, in the oligotrophic Beaufort Sea, may only support a single cohort which increases the susceptibility of the population to the effects of ocean acidification. Contingent on key factors such as stratification and mixing which shape the response of primary producers to on-going changes (Ardyna et al., 2011; Blais et al., 2017), the lengthening of the open-water period due to sea-ice loss and potential increased occurrence of fall phytoplankton blooms (Ardyna et al., 2014) may benefit cohort recruitment and population resilience.

Exposure

Spawning in May or June indicates that larval and juvenile stages are primarily exposed to spring and summer Ω_{ar} conditions whereas adults are more exposed to Ω_{ar} conditions at overwintering depths and under the sea ice. In the Amundsen Gulf, *L. helicina* occurred primarily in the top 50 m (**Figure 4**) comprised of corrosive waters of Pacific origin and Arctic surface waters freshened by sea-ice melt and Mackenzie River inflow. This water column habitat is thus susceptible to seasonal and episodic $\Omega_{ar} < 1$ conditions as well as enhanced acidification (i.e., lower aragonite undersaturation) from the intrusion of anthropogenic CO_2 via air-sea exchange and lateral transport. We hypothesized that dissolution would be highest in areas of upwelling, a known source of undersaturated waters for shelf environments (Feely et al., 2008; Schulz et al., 2019). However, the extent of dissolution was not significantly different between the upwelling, embayment and gateway areas (**Figure 8**), with 83% (2014) and 89.5% (2017) of individuals assessed displaying advanced (Type II or III) shell dissolution. Severe dissolution occurred at every station, indicating that Ω_{ar} dissolution thresholds were surpassed across the entire region. The prevalence of dissolution in the Amundsen Gulf is the highest reported from the natural environment including all the high-latitude habitats reported so far (Bednaršek et al., 2012c, 2014). The proportion of individuals affected by $\Omega_{ar} < 1$ conditions in the Amundsen Gulf is significantly higher than in the Gulf of Alaska or the Bering Sea (Bednaršek et al., submitted). Amundsen Gulf *Limacina* is also more impacted than those in regions of known change. For example, in the California Current ecosystem it is estimated that the incidence of severe shell dissolution due to anthropogenic ocean acidification has doubled in near shore habitats since pre-industrial times yet, on average, only 53% of onshore individuals and 24% of offshore individuals were found to have severe dissolution damage (Bednaršek et al., 2014).

The extent of dissolution was positively correlated with salinity, supporting the notion that Pacific-origin waters are a stronger driver of dissolution than the freshened surface water with reduced buffering capacity (Yamamoto-Kawai et al., 2009; Qi et al., 2017; Zhang et al., 2020). Water conditions near the surface and around the coast (i.e., in embayments) of Amundsen

Gulf are variable due to wind forcing of the ocean. Upwelling and downwelling is particularly evident at Cape Bathurst where it is topographically amplified (Williams and Carmack, 2008), and undersaturated Pacific-origin water can reach the surface during upwelling events. Due to the large response of the coastal ocean to wind forcing, synoptic, seasonal and inter-annual variation in the winds over Amundsen Gulf and the adjacent Beaufort Shelf and Slope will be strong drivers of coastal conditions, including salinity, dissolved nutrients and aragonite saturation state.

Flow along the coast, continental shelf and slope has the potential to move water from far away to the gulf. For example, surface drifters during a downwelling favorable autumn storm traveled along the coast from the Canadian Beaufort Shelf to Darnley Bay in a few days (B. Williams unpublished data). Therefore, pteropods sampled in Amundsen Gulf could have been brought to the gulf by surface oceanic flows and thus conditions experienced on the Beaufort Shelf or slope may have also contributed to their shell dissolution. Exposure to Ω_{ar} undersaturated conditions may also be affected by tidal mixing which has the potential to mix the low-omega, high-nutrient Pacific-origin water with surface waters in shallow regions where tidal flows are amplified. In the study area, regions of potential tidal mixing include the continental shelves on either side of the mouth of Amundsen Gulf, including Cape Bathurst, as well as Dolphin and Union Strait (McLaughlin et al., 2004; Hannah et al., 2009).

Ocean acidification impacts are related to both the magnitude and duration of $\Omega_{ar} < 1$ exposure in natural environments. Pteropod responses are likely based on recurring patterns of exposure, and experimental work suggests that natural populations can exist near their physiological tolerance limit (Bednaršek et al., 2017b). From the 1970s to 2010, the aragonite saturation state has been variable and declining in the upper halocline and deep waters of the Canada Basin and Beaufort Sea (Miller et al., 2014; Zhang et al., 2020). Within this period of decline, an annual (2007–2008) study found that the upper halocline waters of the Amundsen Gulf, between 50 and 150 m depth, had $\Omega_{ar} < 1$ conditions for the entire year except for a short reprieve during June/July (Shadwick et al., 2011). This seasonal persistence of $\Omega_{ar} < 1$ conditions in the halocline is similar to seasonal estimates from the Pacific Arctic region (Cross et al., 2018). In this study, Ω_{ar} conditions (**Figure 3**) were similarly distributed as Shadwick et al. (2011), with saturated conditions occurring in waters <50 m and $\Omega_{ar} < 1$ occurring in the halocline and Atlantic water masses. This indicates that Ω_{ar} undersaturated conditions continue to be a persistent characteristic of the Pacific layer in the Amundsen Gulf and are the result of both natural and anthropogenic sources for the increased CO_2 and lower aragonite saturation state (Ko and Quay, 2020; Zhang et al., 2020). Ongoing monitoring is needed to identify how the saturation state is changing over time and how susceptible species and life stages in the Amundsen Gulf will be affected, with respect to physical damage, physiological impairments, or mortality, by both the magnitude of $\Omega_{ar} < 1$ exposure, and the rate at which Ω_{ar} decreases in coming years.

Although *L. helicina* was located primarily above 50 m at the time of sampling (94–98%, **Figure 4**), it is expected that

L. helicina undergoes diel migrations (Lalli and Gilmer, 1989), suggesting $\Omega_{\text{ar}} < 1$ exposure in the Pacific layer on a daily basis. This regular exposure could explain dissolution at the growing edge. The surface mixed layer represents an important portion of habitat without undersaturated conditions. However, the surface mixed layer can be below or near $\Omega_{\text{ar}} = 1$ for periods of weeks, in the study area, as biological processes lower Ω_{ar} by up to 0.3 in the spring and fall (Chierici et al., 2011) and wind events bring undersaturated waters to the surface episodically. In the central Arctic Ocean, widespread Ω_{ar} undersaturation of surface waters is projected within the next decade due to elevated atmospheric CO_2 (Steinacher et al., 2009) and a similar response to elevated atmospheric CO_2 is projected for the Amundsen Gulf given seasonal warming and freshening as well as lower alkalinity which limits the region's capacity to buffer saturation decreases (Shadwick et al., 2013). Consequently, the surface mixed layer habitat will likely become increasingly corrosive with respect to the magnitude and duration of $\Omega_{\text{ar}} < 1$, thereby increasing pteropod exposure over daily and annual cycles.

Severe dissolution on the first whorl (Figure 7B) indicates that larval pteropods are vulnerable to dissolution, and $\Omega_{\text{ar}} < 1$ conditions due to the remineralization of organic matter can occur when larvae are present in the Amundsen Gulf (Shadwick et al., 2011). Pteropods may over winter at depths > 50 m, similar to key copepod species in the Amundsen Gulf (Darnis and Fortier, 2014). Consequently, hatching and metamorphosis to the juvenile stage could all occur within the undersaturated Pacific halocline where the corrosive Pacific Winter Water resides (Qi et al., 2017; Zhang et al., 2020). Recent under-ice sampling in Darnley Bay, an Amundsen Gulf embayment, measured $\Omega_{\text{ar}} < 1$ near 100 m depth in April, with values 3 m below the sea ice averaging only 1.2 (B. Williams, unpublished data). A dissolution threshold of $\Omega_{\text{ar}} = 1.2$ has been identified for pteropods from other ocean regions (Bednaršek et al., 2019). Although dissolution thresholds have not been experimentally determined for the Amundsen Gulf, it is possible that the larval shell with a thinner or incompletely formed organic layer, is vulnerable to $\Omega_{\text{ar}} > 1$ conditions such that seasonal or even short-term exposure of larvae while at depth, or feeding near the ice, may affect pteropod recruitment and thus interannual variability in *L. helicina* abundance. Annual measurements of Ω_{ar} in the Pacific halocline and surface mixed layer are needed from the study area to advance our understanding of seasonal and episodic occurrences of $\Omega_{\text{ar}} < 1$ conditions.

Shell Modification

This study provides evidence of shell modification in adult individuals sampled in 2014. A homogenous yet unstructured crystalline layer was deposited in patches over damaged areas on the surface of only the first whorl (Figure 9). The shell modification occurred at locations with the most severe dissolution suggesting that the pteropods may have initiated such a process to build a more mechanically durable shell by reducing the porosity or increasing its thickness. Beaufort Sea pteropods naturally build thinner shells in comparison to those from other high latitude habitats (Bednaršek et al., submitted), that could become even thinner under severe dissolution as observed in this

study. More detailed study of the crystalline layer is required to describe the modifications at the nano- or micro-scale of shell building. The unstructured and homogenous layer deposited on the pteropod shells may be similar to reduced crystallographic control of shell formation observed for mussels grown under acidification conditions (Fitzer et al., 2016).

Shell modification as a repair mechanism has been previously documented for *L. helicina* in Arctic waters, characterized as a thickening of the shell caused by the deposition of newly formed aragonite on the inside of the shell (Lischka et al., 2011; Peck et al., 2016, 2018). In this study it is not possible to determine the seasonal timing of the shell modification. It could have occurred during the growth of early life stages, in which case the structurally homogenous crystalline deposition represents a plastic repair response to unfavorable conditions (i.e., lower Ω_{ar} in the spring). Alternatively, it could have deposited under more favorable conditions later in the summer, in which case the unstructured layer would qualify as shell regrowth.

The observed shell modification in 2014, and not in 2017, implies that such deposition is not always feasible and is likely dependent on suitable environmental conditions (Seibel et al., 2012). In 2014, summer phytoplankton concentrations may have provided an adequate, accessible energy source to support shell modification in the absence of other metabolic costs such as reproduction. The absence of the unstructured layer on juvenile shells suggests that energy may have been allocated to growth rather than repair. The shell modification may confer some resilience for damaged adults, and as such potentially allows for higher fitness and better reproductive success.

The shell modification appears to be more of a plastic response to the external environmental conditions, rather than an adaptive response. It is evident that the observed depositions on the first whorl do not constitute a process that would have entirely eliminated the shell dissolution apparent at the individual or population level. Given that the shell modification process was only observed in a few adult individuals at spatially limited locations (e.g., Minto Inlet), regrowth could be an energetically expensive process that organisms will not initiate unless the severity of dissolution is at a critical stage. Nevertheless, under future conditions with lower aragonite undersaturation, it is possible that energy devotion to shell modifications may become more common, or necessary, for survival. If shell modifications are not possible in juveniles, future decreases in aragonite undersaturation may lead to death in early life stages with population and ecosystem consequences.

Ecosystem Linkages

In the Amundsen Gulf, the prevalence and location of dissolution on shells identifies *Limacina* spp. as a sensitive biological indicator of $\Omega_{\text{ar}} < 1$ exposure on a seasonal basis, as proposed for other ocean regions (Bednaršek et al., 2012b, 2017b). Longer periods of monitoring are required to use *Limacina* spp. as a population-level indicator of anthropogenic ocean acidification (IPCC, 2011) given that variability in abundance and distribution is likely related to multiple factors, including the timing of sea-ice opening. Due to ongoing anthropogenic contributions of atmospheric CO_2 , it is predicted that Arctic *L. helicina* will

be unable to form shells by the end of the century (IPCC SRES A2 scenario; Comeau et al., 2012). Tolerances to current rapid rates of change and cumulative perturbation of marine ecosystems are not well known such that the future survival of *Limacina* spp. is uncertain despite apparent resilience to perturbations in the Earth's carbon cycle over evolutionary timescales (Peijnenburg et al., 2019).

Pteropods contribute significantly to marine biogeochemical cycling (Pasternak et al., 2017; Buitenhuis et al., 2019) and are components of zooplankton, fish and seabird diets. On the Canadian Beaufort Shelf, *L. helicina* was found to be a small component of demersal Arctic Cod diets (Majewski et al., 2016), specifically age one fish (Walkusz et al., 2013). *L. helicina* can be a significant part of Pacific Salmon diets, with *L. helicina* abundance explaining 30% of the variability of pink salmon survival in Prince William Sound (Doubleday and Hopcroft, 2015). Dense populations of pteropods in nearshore waters may provide critical energy for juvenile fish. Recent nearshore fish collections in Darnley Bay (2018 and 2019) and near Sachs Harbour (Banks Island, 2018) found *Limacina* sp. in the stomachs of Arctic Char ($n = 4$; <1–13% of diet items), Starry Flounder ($n = 2$; 30–93% of diet items) and Greenland Cod ($n = 1$; 98% of diet items) (D. McNicholl, unpublished data). These results provide evidence that that *L. helicina* are used by Arctic nearshore fishes with different life histories and feeding strategies. The high numbers in some stomachs (100–160 individuals) suggest that *Limacina* sp. may be available in dense populations for nearshore fishes in coastal areas of Amundsen Gulf and are consumed, at minimum, opportunistically. Further studies are needed to assess nearshore distributions of *L. helicina*, e.g., the occurrence of swarms, and the accessibility of pteropods to key life stages of fishes and other predators.

Limacina helicina, as a model indicator, provides direct evidence of combined effects of anthropogenic ocean acidification and other natural processes on aragonite saturation state in the Amundsen Gulf that surpasses other ocean regions. An understanding of food web and other ecosystem consequences (e.g., carbon cycling) requires regional, inter-annual assessments to determine, among other things, pteropod recruitment success relative to the aragonite saturation state over annual cycles. In addition, *L. helicina* provides a warning for other biota with life stages and structures sensitive to calcium carbonate dissolution. Of particular concern is the direct effect of ocean acidification on larval otoliths of near and off-shore fishes in the study area, especially Arctic Cod. *L. helicina*, when treated as a biological indicator, can be an important component of monitoring, and modeling wider ecosystem change related to anthropogenic CO₂ intrusion or cumulative effects of changing atmospheric-ice-ocean interactions.

CONCLUSION

The prevalence of dissolution observed in this study indicates the presence of $\Omega_{ar} < 1$ conditions under the sea ice when larval *L. helicina* were present, as well as during open-water periods when dissolution occurred along the growing edge of

shells. The timing of sea-ice opening may be a key driver of the interannual variability in *L. helicina* abundance. However, sea ice and resource variability did not appear to affect the wide spread occurrence and observed severity of dissolution. The seasonal persistence of $\Omega_{ar} < 1$ in the Pacific layer suggests that this *L. helicina* habitat in the Amundsen Gulf is largely corrosive and populations possibly function near their tolerance level such that some adult individuals can initiate shell modifications upon the most severe dissolution conditions if resources are adequate and available. The energetic balance between shell modification and growth needs to be better understood to determine the response of *L. helicina* populations to variable environmental conditions, and the follow-on consequences for the ecosystem.

Past occurrence and recent trends in shell dissolution are not currently known for the Beaufort Shelf or the Amundsen Gulf. It is expected that dissolution has been augmented by enhanced acidification over the last 20 years. Changes in Pacific winter waters are currently driving the rapid expansion (i.e., area and depth) of ocean acidification in the western Arctic Ocean (Qi et al., 2017) and the Canadian Beaufort shelf remains vulnerable to changes in the volume and freshwater content of Pacific waters, upwelling of undersaturated waters, as well as the intrusion of atmospheric CO₂ over a lengthening open-water period. Given the ecological importance of *L. helicina* in the Canadian Arctic, the inclusion of *L. helicina* as an indicator species in offshore and coastal programs will inform the severity of biological responses to ongoing ocean acidification. The severe occurrence of dissolution indicates that other vulnerable species and life stages should also be assessed.

DATA AVAILABILITY STATEMENT

The raw data supporting the conclusions of this article will be made available by the authors, without undue reservation.

AUTHOR CONTRIBUTIONS

AN conducted the field work and drafted the manuscript. AN and WWa contributed the zooplankton data. NB contributed the SEM analyses. WWi contributed the oceanographic data. CM and KA-S contributed the chemistry data. JR was the BREA program lead and RF led program collaborations, both provided expert input. All authors participated in the writing of the manuscript and approved the submitted version.

FUNDING

AN, CM, and KA-S were supported by the Aquatic Climate Change Adaptation Services Program, Fisheries and Oceans Canada. RF was supported by the NOAA Ocean Acidification Program and the Pacific Marine Environmental Laboratory. This is contribution number 5128 from the NOAA Pacific Marine Environmental Laboratory. Financial support for the

BREA-MFP and CBS-MEA programs was provided by Fisheries and Oceans Canada (Rotational Fund, Northern Contaminants Program, Marine Conservation Targets, International Governance Strategy), Environmental Studies Research Fund (NRCAN), the Beaufort Regional Environmental Assessment (AANDC), and the Beaufort Regional Strategic Environmental Assessment (CIRNAC).

ACKNOWLEDGMENTS

We acknowledge the excellent support of the captains and crew of the *FV Frosti* and the staff at Frosti Fishing

Inc. We appreciate the leadership of all the chief scientists during the BREA-MFP and CBS-MEA. Field collections were supported by J. Eert, H. Maclean, S. Zimmerman, M. Dempsey, G. Meisterhans, R. Husserr, S. MacPhee, A. Sastri, K. Young, and A. Timmerman. Coastal fish collection was supported by community monitors from Paulatuk and Sachs Harbour NT. A. Burt processed the 2017 pteropod taxonomy samples, S. Punshon performed DIC and TA analyses and J. Charette prepared the omega database. E. Ipsen, A. Ehrman, and M. Ouellette provided manuscript support. We are grateful to the Inuvialuit Game Council for supporting this project and for providing valuable input to the study design and logistics.

REFERENCES

- AMAP (2018). *AMAP Assessment 2018: Arctic Ocean Acidification*. Tromsø: Arctic Monitoring and Assessment Programme (AMAP), vi+187.
- Ardyna, M., Babin, M., Gosselin, M., Devred, E., Rainville, L., and Tremblay, J. -É (2014). Recent Arctic Ocean sea ice loss triggers novel fall phytoplankton blooms. *Geophys. Res. Lett.* 41, 6207–6212. doi: 10.1002/2014GL061047
- Ardyna, M., Gosselin, M., Michel, C., Poulin, M., and Tremblay, J. -É (2011). Environmental forcing of phytoplankton community structure and function in the Canadian High Arctic: contrasting oligotrophic and eutrophic regions. *Mar. Ecol. Prog. Ser.* 442, 37–47. doi: 10.3354/meps09378
- Azetsu-Scott, K., Clarke, A., Falkner, K., Hamilton, J., Jones, E. P., Lee, C., et al. (2010). Calcium carbonate saturation states in the waters of the Canadian Arctic Archipelago and the Labrador Sea. *J. Geophys. Res.* 115:C11021. doi: 10.1029/2009JC005917
- Azetsu-Scott, K., Starr, M., Mei, Z.-P., and Granskog, M. (2014). Low calcium carbonate saturation state in an Arctic inland sea having large and varying fluvial inputs: the Hudson Bay system. *J. Geophys. Res. Oceans* 119, 6210–6220. doi: 10.1002/2014JC009948
- Bednaršek, N., Feely, R. A., Howes, E. L., Hunt, B. P. V., Kessouri, F., León, P., et al. (2019). Systematic review and meta-analysis toward synthesis of thresholds of ocean acidification impacts on calcifying pteropods and interactions with warming. *Front. Mar. Sci.* 6:227. doi: 10.3389/fmars.2019.00227
- Bednaršek, N., Feely, R. A., Reum, J. C. P., Peterson, B., Menkel, J., Alin, S., et al. (2014). *Limacina helicina* shell dissolution as an indicator of declining habitat suitability owing to ocean acidification in the California Current Ecosystem. *Proc. R. Soc. B Biol. Sci.* 281:20140123. doi: 10.1098/rspb.2014.0123
- Bednaršek, N., Feely, R. A., Tolimieri, N., Hermann, A. J., Siedlecki, S. A., Waldbusser, G. G., et al. (2017a). Exposure history determines pteropod vulnerability to ocean acidification along the US West Coast. *Sci. Rep.* 7:4526. doi: 10.1038/s41598-017-03934-z
- Bednaršek, N., Klinger, T., Harvey, C. J., Weisberg, S., McCabe, R. M., Feely, R. A., et al. (2017b). New ocean, new needs: application of pteropod shell dissolution as a biological indicator for marine resource management. *Ecol. Indic.* 76, 240–244. doi: 10.1016/j.ecolind.2017.01.025
- Bednaršek, N., Možina, J., Vogt, M., O'Brien, C., and Tarling, G. A. (2012a). The global distribution of pteropods and their contribution to carbonate and carbon biomass in the modern ocean. *Earth Syst. Sci. Data* 4, 167–186. doi: 10.5194/essd-4-167-2012
- Bednaršek, N., Naish, K., Feely, R. A., Hauri, C., Kimoto, K., Hermann, A. J., et al. (submitted). Integrated assessment of the risks to ocean acidification in the Northern high latitudes: regional comparison of exposure, sensitivity and adaptive capacity of pelagic calcifiers. *Front. Mar. Sci.*
- Bednaršek, N., Tarling, G. A., Bakker, D. C. E., Fielding, S., Cohen, A., Kuzirian, A., et al. (2012b). Description and quantification of pteropod shell dissolution: a sensitive bioindicator of ocean acidification. *Glob. Change Biol.* 18, 2378–2388. doi: 10.1111/j.1365-2486.2012.02668.x
- Bednaršek, N., Tarling, G. A., Fielding, S., and Baker, D. C. E. (2012c). Population dynamics and biogeochemical significance of *Limacina helicina Antarctica* in the Scotia sea (Southern Ocean). *Deep Sea Res. II* 59–60, 105–116. doi: 10.1016/j.dsr2.2011.08.003
- Blais, M., Ardyna, M., Gosselin, M., Dumont, D., Bélanger, S., Éric, J., et al. (2017). Contrasting interannual changes in phytoplankton productivity and community structure in the coastal Canadian Arctic Ocean. *Limnol. Oceanogr.* 62, 2480–2497. doi: 10.1002/lno.1058
- Buitenhuis, E. T., Le Quéré, C., Bednaršek, N., and Schiebel, R. (2019). Large contribution of pteropods to shallow CaCO₃ export. *Global Biogeochem. Cycles* 33, 458–468. doi: 10.1029/2018GB006110
- Busch, D. S., Maher, M., Thibodeau, P., and McElhany, P. (2014). Shell condition and survival of Puget Sound pteropods are impaired by ocean acidification conditions. *PLoS One* 9:e105884. doi: 10.1371/journal.pone.0105884
- Carmack, E. C., and MacDonald, R. W. (2002). Oceanography of the Canadian shelf of the Beaufort Sea: a setting for marine life. *Arctic* 55, 29–45.
- Chierici, M., Fransson, A., Lansard, B., Miller, L. A., Mucci, A., Shadwick, E., et al. (2011). The impact of biogeochemical processes and environmental factors on the calcium carbonate saturation state in the circumpolar flow lead in the Amundsen Gulf, Arctic Ocean. *J. Geophys. Res.* 116:C00G09. doi: 10.1029/2011JC007184
- Comeau, S., Gattuso, J.-P., Nisumaa, A.-M., and Orr, J. (2012). Impact of aragonite saturation state changes on migratory pteropods. *Proc. R. Soc. B* 279, 732–738. doi: 10.1098/rspb.2011.0910
- Comeau, S., Jefferee, R., Teyssié, J.-L., and Gattuso, J.-P. (2010). Response of the Arctic pteropod *Limacina helicina* to projected future environmental conditions. *PLoS One* 5:e11362. doi: 10.1371/journal.pone.0011362
- Cross, J. N., Mathis, J. T., Pickart, R. S., and Bates, N. R. (2018). Formation and transport of corrosive water in the Pacific Arctic region. *Deep Sea Res.* 152, 67–81. doi: 10.1016/j.dsr2.2018.05.020
- Darnis, G., Barber, D. G., and Fortier, L. (2008). Sea ice and the onshore-offshore gradient in pre-winter zooplankton assemblages in southeastern Beaufort Sea. *J. Mar. Syst.* 74, 994–1011. doi: 10.1016/j.jmarsys.2007.09.003
- Darnis, G., and Fortier, L. (2014). Temperature, food and the seasonal vertical migration of key arctic copepods in the thermally stratified Amundsen Gulf (Beaufort Sea, Arctic Ocean). *J. Plankton Res.* 36, 1092–1108. doi: 10.1093/plankt/fbu035
- Dickson, A. G., Sabine, C. L., and Christian, J. R. (eds). (2007). *Guide to Best Practices for Ocean CO₂ Measurements*. PICES Special Publication. Sidney, NSW: North Pacific Marine Science Organization, Vol. 3, 191.
- Doubleday, A. J., and Hopcroft, R. R. (2015). Interannual patterns during spring and late summer of larvaceans and pteropods in the coastal Gulf of Alaska, and their relationship to pink salmon survival. *J. Plankton Res.* 37, 134–150. doi: 10.1093/plankt/fbu092
- Fabry, V. J., McClintock, J. B., Mathis, J. T., and Grebmeier, J. M. (2009). Ocean acidification at high latitudes: the bellwether. *Oceanography* 22, 160–171. doi: 10.5670/oceanog.2009.105
- Fabry, V. J., Seibel, B. A., Feely, R. A., and Orr, J. C. (2008). Impacts of ocean acidification on marine fauna and ecosystem processes. *ICES J. Mar. Sci.* 65, 414–432. doi: 10.1093/icesjms/fsn048

- Feely, R. A., Alin, S., Carter, B., Bednaršek, N., Hales, B., Chan, F., et al. (2016). Chemical and biological impacts of ocean acidification along the west coast of North America. *Estuar. Coast. Shelf Sci.* 183, 260–270. doi: 10.1016/j.ecss.2016.08.043
- Feely, R. A., Sabine, C. L., Hernandez-Ayon, J. M., Ianson, D., and Hales, B. (2008). Evidence for upwelling of corrosive "acidified" water onto the continental shelf. *Science* 320, 1490–1492. doi: 10.1126/science.1155676
- Fitzer, S., Chung, P., Maccherozzi, F., Dhesi, S. S., Kamenos, N. A., Phoenix, V. R., et al. (2016). Biomineral shell formation under ocean acidification: a shift from order to chaos. *Sci. Rep.* 6:21076. doi: 10.1038/srep21076
- Forest, A., Tremblay, J. -É., Gratton, Y., Martin, J., Gagnon, J., Darnis, G., et al. (2011). Biogenic carbon flow pathways in the planktonic food web of the Amundsen Gulf (Arctic Ocean): a synthesis of field measurements and inverse modeling analyses. *Prog. Oceanogr.* 91, 410–436. doi: 10.1016/j.pcean.2011.05.002
- Gannefors, C., Böer, M., Kattner, G., Graeve, M., Eiane, K., Gulliksen, B., et al. (2005). The Arctic sea butterfly *Limacina helicina*: lipids and life strategy. *Mar. Biol.* 147, 169–177. doi: 10.1007/s00227-004-1544-y
- Gardner, J., Manno, C., Bakker, D. C. E., Peck, V. L., and Tarling, G. A. (2018). Southern Ocean pteropods at risk from ocean warming and acidification. *Mar. Biol.* 165:8. doi: 10.1007/s00227-017-3261-3
- Gilmer, R. W., and Harbison, G. R. (1991). Diet of *Limacina helicina* (Gastropoda: thecosomata) in Arctic waters in midsummer. *Mar. Ecol. Prog. Ser.* 77, 125–134.
- Hannah, C. G., Dupont, F., and Dunphy, M. (2009). Polynyas and tidal currents in the Canadian Arctic Archipelago. *Arctic* 62, 83–95.
- Haradsson, C., Anderson, L. G., Hasselöv, M., Hulth, S., and Olsson, K. (1997). Rapid high-precision potentiometric titration of alkalinity in ocean and sediment pore waters. *Deep Sea Res. Part I* 44, 2031–2044.
- IPCC (2011). "Workshop report of the intergovernmental panel on climate change workshop on impacts of ocean acidification on marine biology and ecosystems," in *IPCC Working Group II Technical Support Unit*, eds C. B. Field, V. Barros, T. F. Stocker, D. Qin, K. J. Mach, G.-K. Plattner, et al. (Stanford, CA: Carnegie Institution), 164.
- Johnson, K. M., King, A. E., and Mc Sieburth, M. (1985). Coulometric TCO₂ analyses for marine studies: an introduction. *Mar. Chem.* 16, 61–82.
- Kirilov, S., Dmitrenko, I., Tremblay, B., Gratton, Y., Barber, D., and Rysgaard, S. (2016). Upwelling of Atlantic water along the Canadian Beaufort Sea continental slope: favorable atmospheric conditions and seasonal and interannual variations. *J. Clim.* 29, 4509–4523. doi: 10.1175/jcli-d-15-0804.1
- Klok, C., Wijsman, J. W. M., Kaag, K., and Foekema, E. (2014). Effects of CO₂ enrichment on cockle shell growth interpreted with a dynamic energy budget model. *J. Sea Res.* 94, 111–116. doi: 10.1016/j.seares.2014.01.011
- Ko, Y., and Quay, P. (2020). Origin and accumulation of an anthropogenic CO₂ and ¹³C Suess effect in the Arctic Ocean. *Global Biogeochem. Cycle* 34:e2019GB006423. doi: 10.1029/2019GB006423
- Kobayashi, H. A. (1974). Growth cycle and related vertical distribution of the thecosomatous pteropod *Spiratella* ("*Limacina*") *helicina* in the central Arctic Ocean. *Mar. Biol.* 26, 295–301. doi: 10.1007/BF00391513
- Kohlbach, D., Graeve, M., Lange, B., David, C., Peeken, I., and Flores, H. (2016). The importance of ice algae-produced carbon in the central Arctic Ocean ecosystem: food web relationships revealed by lipid and stable isotope analyses. *Limnol. Oceanogr.* 61, 2027–2044. doi: 10.1002/lno.10351
- Kohlbach, D., Graeve, M., Lange, B., David, C., Schaafsma, F. L., van Franeker, J. A., et al. (2018). Dependency of Antarctic zooplankton species on ice algae-produced carbon suggests a sea ice-driven pelagic ecosystem during winter. *Glob. Change Biol.* 24, 4667–4681. doi: 10.1111/gcb.14392
- Kroeker, K. J., Kordas, R. L., Crim, R., Hendriks, I. E., Ramajo, L., Singh, G. S., et al. (2013). Impacts of ocean acidification on marine organisms: quantifying sensitivities and interaction with warming. *Glob. Change Biol.* 19, 1884–1896. doi: 10.1111/gcb.12179
- Lalli, C. M., and Gilmer, R. W. (1989). *Pelagic Snails: The Biology of Holoplanktonic Gastropod Mollusks*. Stanford, CA: Stanford University Press.
- Lee, K., Kim, T. -W., Byrne, R. H., Millero, F. J., Feely, R. A., and Liu, Y. -M. (2010). The universal ratio of boron to chlorinity for the North Pacific and North Atlantic oceans. *Geochim. Cosmochim. Acta* 74, 1801–1811. doi: 10.1016/j.gca.2009.12.027
- Lewis, E., and Wallace, D. W. R. (1998). *Program Developed for CO₂ Systems Calculations, ORNL/CDIAC-105, Carbon Dioxide Info. Anal. Cent.* Oak Ridge, TN: Oak Ridge National Laboratory.
- Lischka, S., Büdenbender, J., Boxhammer, T., and Riebesell, U. (2011). Impact of ocean acidification and elevated temperatures on early juveniles of the polar shelled pteropod *Limacina helicina*: mortality, shell degradation, and shell growth. *Biogeosciences* 8, 919–932. doi: 10.5194/bg-8-919-2011
- Long, W. C., Swiney, K. M., Harris, C., Page, H. N., and Foy, R. J. (2013). Effects of Ocean Acidification on Juvenile Red King Crab (*Paralithodes camtschaticus*) and Tanner Crab (*Chionoecetes bairdi*) Growth, Condition, Calcification, and Survival. *PLoS One* 8:e60959. doi: 10.1371/journal.pone.0060959
- Lueker, T. J., Dickson, A. G., and Keeling, C. D. (2000). Ocean pCO₂ calculated from dissolved inorganic carbon, alkalinity, and equations for K₁ and K₂: validation based on laboratory measurements of CO₂ in gas and seawater at equilibrium. *Mar. Chem.* 70, 105–119. doi: 10.1016/S0304-4203(00)00022-0
- Majewski, A. R., Walkusz, W., Lynn, B. R., Atchison, S., Eert, J., and Reist, J. D. (2016). Distribution and diet of demersal Arctic Cod, *Boreogadus saida*, in relation to habitat characteristics in the Canadian Beaufort Sea. *Polar Biol.* 39, 1087–1098. doi: 10.1007/s00300-015-1857-y
- Martin, J., Tremblay, J. E., Gagnon, J., Tremblay, G., Lapoussiere, A., Jose, C., et al. (2010). Prevalence, structure and properties of subsurface chlorophyll maxima in Canadian Arctic waters. *Mar. Ecol. Prog. Ser.* 412, 69–84. doi: 10.3354/meps08666
- Mathis, J. T., Byrne, R. H., McNeil, C. L., Pickart, R. P., Juranek, L., Moore, G. W. K., et al. (2012). Storm-induced upwelling of high pCO₂ waters onto the continental shelf of the western Arctic Ocean and implications for carbonate mineral saturation states. *Geophys. Res. Lett.* 39:L07606. doi: 10.1029/2012GL051574
- Mathis, J. T., Cross, J. N., Evans, W., and Doney, S. C. (2015). Ocean acidification in the surface waters of the Pacific-Arctic boundary regions. *Oceanography* 28, 122–135. doi: 10.5670/oceanog.2015.36
- McLaughlin, F. A., Carmack, E. C., Ingram, R. G., Williams, W. J., and Michel, C. (2004). "Oceanography of the northwest passage," in *The Sea: The Global Coastal Ocean*, Vol. 14B, eds R. Robinson and K. H. Brink (Cambridge, MA: Harvard University Press), 1211–1236.
- Michel, C., Legendre, L., Ingram, R. G., Gosselin, M., and Levasseur, M. (1996). Carbon budget of ice algae under first-year ice: evidence of a significant transfer to zooplankton grazers. *J. Geophys. Res.* 101, 18345–18360. doi: 10.1029/96JC00045
- Miller, L. A., Macdonald, R. W., McLaughlin, F., Mucci, A., Yamamoto-Kawai, M., Giesbrecht, K. E., et al. (2014). Changes in the marine carbonate system of the western Arctic: patterns in a rescued data set. *Polar Res.* 33:20577. doi: 10.3402/polar.v33.20577
- Mol, J., Thomas, H., Myers, P. G., Hu, X., and Mucci, A. (2018). Inorganic carbon fluxes on the Mackenzie Shelf of the Beaufort Sea. *Biogeosciences* 15, 1011–1027. doi: 10.5194/bg-15-1011-2018
- Mundy, C. J., Gosselin, M., Ehn, J., Gratton, Y., Rossnagel, A., Barber, D. G., et al. (2009). Contribution of under-ice primary production to an ice-edge upwelling phytoplankton bloom in the Canadian Beaufort Sea. *Geophys. Res. Lett.* 36:L17601. doi: 10.1029/2009gl038837
- Niemi, A., Majewski, A., Archambault, P., Atchison, S., Cypihot, V., Eert, J., et al. (2020). *Data from the BREA-MFP and CBS-MEA Research Programs Describing the Anguniaqvia niqiqyuam Marine Protected Area (ANMPA) Ecosystem*. Canadian Data Report of Fisheries and Aquatic Sciences 1316, ix + 91. Ottawa: Fisheries and Oceans Canada
- Nishizawa, Y., Sasaki, H., and Takahashi, K. (2016). Interannual variability in shelled pteropods (*Limacina* spp.) in the Indian sector of the Southern Ocean during austral summer. *Antarct. Res. Commun.* 60, 35–48. doi: 10.15094/00012672
- Ou, M., Hamilton, T. J., Eom, J., Lyall, E. M., Gallup, J., Jiang, A., et al. (2015). Responses of pink salmon to CO₂-induced aquatic acidification. *Nat. Clim. Change* 5, 950–955. doi: 10.1038/nclimate2694
- Parsons, T. R., Maita, Y., and Lalli, C. M. (1984). *A Manual of Chemical and Biological Methods for Seawater Analysis*. Oxford: Pergamon Press.
- Pasternak, A. F., Drits, A. V., and Flint, M. V. (2017). Feeding, egg production, and respiration rate of pteropods *Limacina* in Arctic seas. *Oceanology* 57, 122–129. doi: 10.1134/s000143701701012x

- Peck, V. L., Oakes, R. L., Harper, E. M., Manno, C., and Tarling, G. A. (2018). Pteropods counter mechanical damage and dissolution through extensive shell repair. *Nat. Commun.* 9:264. doi: 10.1038/s41467-017-02692-w
- Peck, V. L., Tarling, G. A., Manno, C., Harper, E. M., and Tynan, E. (2016). Outer organic layer and internal repair mechanism protects pteropod *Limacina helicina* from ocean acidification. *Deep Sea Res.* 127, 41–52. doi: 10.1016/j.dsr2.2015.12.005
- Peijnenburg, K. T. C. A., Janssen, A. W., Wall-Palmer, D., Goetze, E., Maas, A., Jonathan, A. D., et al. (2019). The origin and diversification of pteropods predate past perturbations in the Earth's carbon cycle. *bioRxiv* [preprint] doi: 10.1101/813386
- Peng, G., Steele, M., Bliss, A. C., Meier, W. N., and Dickinson, S. (2018). Temporal means and variability of arctic sea ice melt and freeze season climate indicators using a satellite climate data record. *Remote Sens.* 10:1328. doi: 10.3390/rs10091328
- Qi, D., Chen, L., Chen, B., Gao, A., Zhong, W., Feely, R. A., Anderson, L. G., et al. (2017). Increase in acidifying water in the western Arctic Ocean. *Nat. Clim. Change* 7, 195–199. doi: 10.1038/nclimate3228
- Riedel, A., Michel, C., Gosselin, M., and LeBlanc, B. (2008). Winter-spring dynamics in sea-ice carbon cycling in the coastal Arctic Ocean. *J. Mar. Syst.* 74, 918–932. doi: 10.1016/j.jmarsys.2008.01.003
- Robbins, L. L., Wynn, J. G., Lisle, J. T., Yates, K. K., Knorr, P. O., Byrne, R. H., et al. (2013). Baseline monitoring of the western Arctic Ocean estimates 20% of Canadian Basin surface waters are undersaturated with respect to aragonite. *PLoS One* 8:e73796. doi: 10.1371/journal.pone.0073796
- Róžańska, M., Gosselin, M., Poulin, M., Wiktor, J. M., and Michel, C. (2009). Influence of environmental factors on the development of bottom landfast ice protists in the Canadian Beaufort Sea during the winter-spring transition. *Mar. Ecol. Prog. Ser.* 386, 43–59. doi: 10.3354/meps08092
- Sallon, A., Michel, C., and Gosselin, M. (2011). Summertime primary production and carbon export in the southeastern Beaufort Sea during the low ice year of 2008. *Polar Biol.* 34, 1989–2005. doi: 10.1007/s00300-011-1055-5
- Sato-Okoshi, W., Okoshi, K., Sasaki, H., and Akiha, F. (2010). Shell structure of two polar pelagic molluscs, Arctic *Limacina helicina* and Antarctic *Limacina helicina antarctica* forma *antarctica*. *Polar Biol.* 33, 1577–1583. doi: 10.1007/s00300-010-0849-1
- Schulz, K. G., Hartley, S., and Eyre, B. (2019). Upwelling amplifies ocean acidification on the east Australian shelf: implications for marine ecosystems. *Front. Mar. Sci.* 6:636. doi: 10.3389/fmars.2019.00636
- Seibel, B. A., Maas, A. E., and Dierssen, H. M. (2012). Energetic plasticity underlies a variable response to ocean acidification in the pteropod, *Limacina helicina antarctica*. *PLoS One* 7:e30464. doi: 10.1371/journal.pone.0030464
- Sévigny, C., Gratton, Y., and Galbraith, P. S. (2015). Frontal structures associated with coastal upwelling and ice-edge subduction events in southern Beaufort Sea during the Canadian Arctic Shelf exchange study. *J. Geophys. Res. Oceans* 120, 2523–2539. doi: 10.1002/2014jc010641
- Shadwick, E. H., Thomas, H., Chierici, M., Else, B., Fransson, A., Michel, C., et al. (2011). Seasonal variability of the inorganic carbon system in the Amundsen Gulf region of the southeastern Beaufort Sea. *Limnol. Oceanogr.* 56, 303–322. doi: 10.4319/lo.2011.56.1.0303
- Shadwick, E. H., Trull, T. W., Thomas, H., and Gibson, J. A. E. (2013). Vulnerability of polar oceans to anthropogenic acidification: comparison of Arctic and Antarctic seasonal cycles. *Sci. Rep.* 3:2339.
- Smoot, C. A., and Hopcroft, R. R. (2017). Cross-shelf gradients of epipelagic zooplankton communities of the Beaufort Sea and the influence of localized hydrographic features. *J. Plankton Res.* 39, 65–78. doi: 10.1093/plankt/fbw080
- Stasko, A., Swanson, H., Atchison, S., MacPhee, S., Majewski, A., de Montety, L., et al. (2017). *Stable Isotope Data ($\delta^{15}N$, $\delta^{13}C$) for Marine Fishes and Invertebrates from the Beaufort Regional Environmental Assessment Marine Fishes Project, August–September 2012 and 2013*. Canadian Data Report of Fisheries and Aquatic Sciences 1270, vi + 63. Ottawa: Fisheries and Oceans Canada
- Steinacher, M., Joos, F., Frölicher, T. L., Plattner, G. K., and Doney, S. C. (2009). Imminent ocean acidification in the Arctic projected with the NCAR global coupled carbon cycle-climate model. *Biogeosciences* 6, 515–533. doi: 10.5194/bg-6-515-2009
- Tremblay, J. -É., Bélanger, S., Barber, D. G., Asplin, M., Martin, J., Darnis, G., et al. (2011). Climate forcing multiplies biological productivity in the coastal Arctic Ocean. *Geophys. Res. Lett.* 38:L18604. doi: 10.1029/2011GL048825
- Van Guelpen, L., Markle, D. F., and Duggan, D. J. (1982). An evaluation of accuracy, precision, and speed of several zooplankton sub-sampling techniques. *J. Cons. Int. Explor. Mer.* 40, 226–236.
- Walkusz, W., Paulić, J. E., Kwaśniewski, S., Williams, W. J., Wong, S., and Papst, M. H. (2010). Distribution, diversity and biomass of summer zooplankton from the coastal Canadian Beaufort Sea. *Polar Biol.* 33, 321–335. doi: 10.1007/s00300-009-0708-0
- Walkusz, W., Williams, W. J., and Kwasniewski, S. (2013). Vertical distribution of mesozooplankton in the coastal Canadian Beaufort Sea in summer. *J. Mar. Syst.* 127, 26–35. doi: 10.1016/j.jmarsys.2012.01.001
- Wang, K., Hunt, B. P. V., Liang, C., Pauly, D., Pakhomov, E. A. (2017). Reassessment of the life cycle of the pteropod *Limacina helicina* from a high resolution interannual time series in the temperate North Pacific. *ICES J. Mar. Sci.* 74, 1906–1920. doi: 10.1093/icesjms/fsx014
- Williams, C. R., Dittman, A. H., McElhany, P., Busch, D. S., Maher, M. T., Bammler, T. K., et al. (2019). Elevated CO₂ impairs olfactory-mediated neural and behavioral responses and gene expression in ocean-phase coho salmon (*Oncorhynchus kisutch*). *Glob Change Biol.* 25, 963–977. doi: 10.1111/gcb.14532
- Williams, W. J., and Carmack, E. C. (2008). Combined effect of wind-forcing and isobath divergence on upwelling at Cape Bathurst. *Beaufort Sea. J. Mar. Res.* 66, 645–663. doi: 10.1357/002224008787536808
- Yamamoto-Kawai, M., McLaughlin, F. A., Carmack, E. C., Nishino, S., and Shimada, K. (2009). Aragonite undersaturation in the Arctic Ocean: effects of ocean acidification and sea ice melt. *Science* 326, 1098–1100. doi: 10.1126/science.1174190
- Zhang, Y., Yamamoto-Kawai, M., and Williams, W. J. (2020). Two decades of ocean acidification in the surface waters of the Beaufort Gyre, Arctic Ocean: effects of sea ice melt and retreat from 1997–2016. *Geophys. Res. Lett.* 47:e60119. doi: 10.1029/2019GL086421

Conflict of Interest: The authors declare that the research was conducted in the absence of any commercial or financial relationships that could be construed as a potential conflict of interest.

Copyright © 2021 Niemi, Bednaršek, Michel, Feely, Williams, Azetsu-Scott, Walkusz and Reist. This is an open-access article distributed under the terms of the Creative Commons Attribution License (CC BY). The use, distribution or reproduction in other forums is permitted, provided the original author(s) and the copyright owner(s) are credited and that the original publication in this journal is cited, in accordance with accepted academic practice. No use, distribution or reproduction is permitted which does not comply with these terms.